

## Supplementary Materials

# Ordered and Disordered Microstructures of Nanoconfined Conducting Polymers

*Sukanya Das,<sup>1</sup> Pranay Venkatesh,<sup>2</sup> Sarbani Ghosh,<sup>2</sup> K. S. Narayan<sup>1,\*</sup>*

<sup>1</sup>Chemistry and Physics of Materials Unit and School of Advanced Materials, Jawaharlal Nehru Centre for Advanced Scientific Research, Bengaluru- 560064, India.

<sup>2</sup>Department of Chemical Engineering, Birla Institute of Technology and Science (BITS), Pilani Campus, Rajasthan- 333031, India

\*Email: narayan@jncastr.ac.in

### List of contents:

1. (i) XPS and EPR of PEDOT:PSS with varying PSS content, (ii) Calculation of the effective number of nanochannels in electrical conduction.
2. HRTEM images of PEDOT:PSS at a tilt angle: cross section view
3. A. HRTEM images of bulk films of PEDOT:Tos, PEDOT:PSS in spin coated, drop casted methods, PEDOT:PSS with variation in PSS part: PH1000 (1:2.5), A14083 (1:6) grades, PEDOT:PSS mix (1:4.83) and acid treated PEDOT films
4. HRTEM images of PEDOT:PSS and PEDOT:Tos in different nanochannels of channel diameters 20 nm, 50 nm, 80 nm and 100 nm.
5. Surface morphology of acid treated PEDOT:PSS surfaces
6. Atomic force spectroscopy
7. MD simulation results

1. X-ray photoelectron spectroscopy XPS and Electron paramagnetic resonance EPR signal of (i) PEDOT:PSS with varying PSS content and (ii) PEDOT:Tos

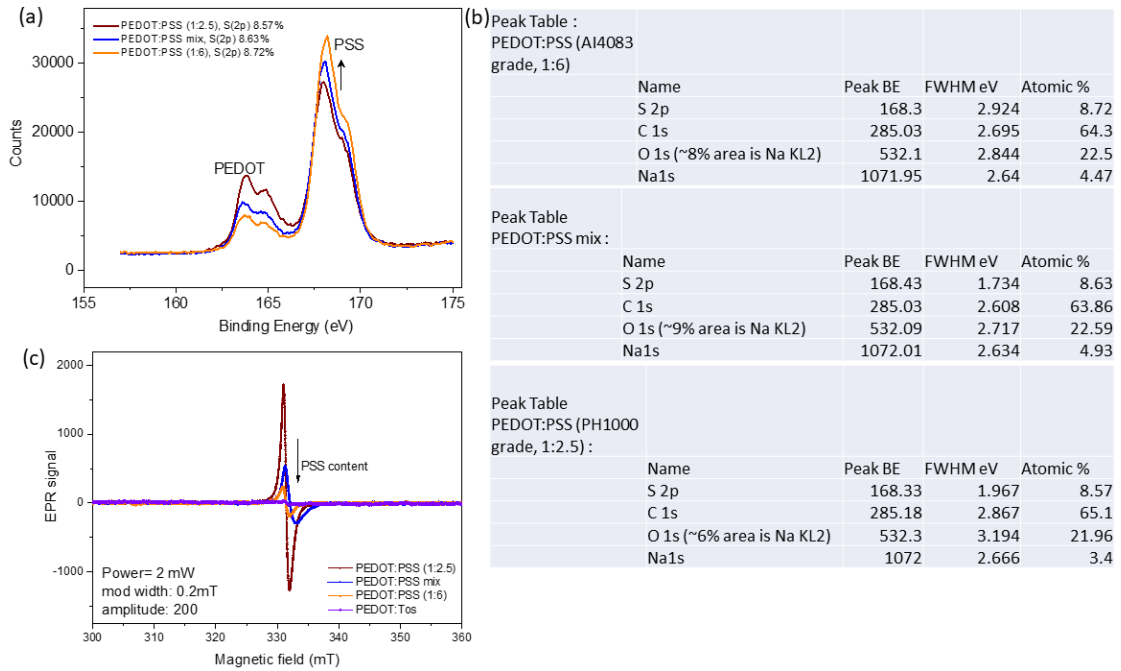
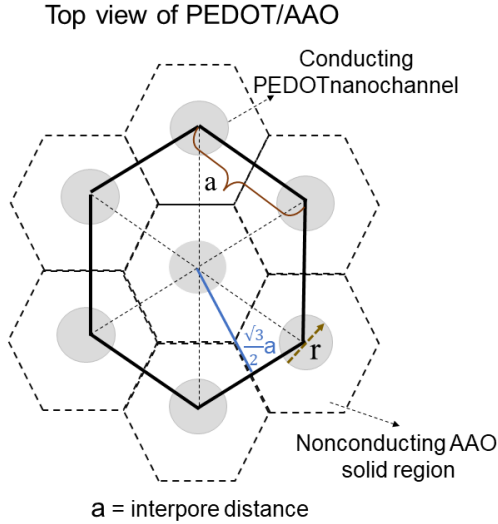


Figure S1: (a) XPS\_S2p and (b) peak table values of each components of PEDOT:PSS. (c) EPR of PEDOT:PSS along with the PSS variation and PEDOT:Tos.

Figure S1(a) shows the S(2p) XPS spectra of PEDOT:PSS films with two signal bands (i) one band between 166 and 172 eV which is assigned to the signal from the sulfur atoms of PSS and (ii) other band between 162 and 166 eV with doublet peaks is usually attributed to the sulfur atoms of PEDOT part. The intensity increases with increasing PSS ratio in the shaded band in the figure(a). EPR signal detects the presence of unpaired electrons and the peak is gradually suppressed due to increase to PSS content in PEDOT:PSS. PEDOT:Tos on the other hand detects nearly no EPR signal which is consistent with previous literature reports, indicating that polaron pairs or bipolarons are the only type of charge carriers.

(ii) Calculation of the effective number of nanochannels in electrical conduction.

The figure below shows the top view of PEDOT/AAO surface with channel diameter= $r$  and inter channel distance= $a$ .



The hexagon in solid line represents one-unit cell.

Therefore, total no. of pores in hexagon = 1 nanochannel at center + ( $\frac{1}{3} * 6$  corner channels)  
 = 1+2 = 3 channels

Area of conducting PEDOT regions in the unit cell =  $3 * \pi * (\frac{r}{2})^2$

Total area of unit cell (conducting channels+ solid walls) =  $6 * \text{area of each equilateral triangles}$   
 $= 6 * \frac{\sqrt{3}}{4} a^2$  unit sq. =  $3 \frac{\sqrt{3}}{2} a^2$  unit sq.

Therefore, the fractional overlapping area of pores =  $\frac{\text{The contributing area from pores}}{\text{Total area (pores+walls)}} = \frac{3\pi(\frac{r}{2})^2}{3\frac{\sqrt{3}}{2}a^2}$

Thus,  $A_{\text{frac}} = \frac{2\pi(\frac{r}{2})^2}{\sqrt{3}a^2} = \frac{2\pi(\text{Pore radius})^2}{\sqrt{3}(\text{Inter-pore dia})^2}$

If the overlapping area be =  $1 \text{ mm}^2$ , then unused area =  $[1 - \frac{2\pi(\frac{r}{2})^2}{\sqrt{3}a^2}] \text{ mm}^2$

Thus, for 20 nm PEDOT/AAO, where  $r=20$  nm,  $a=65$  nm, unused area%=91.41%.

## 2. HRTEM analysis of PEDOT:PSS (at a tilt angle of TEM carbon grid)

Crystalline ordered domains are observed from the walls of nanochannels by tilting the carbon grid at 10 deg. This gives an idea of cross-sectional view of the nanochannels (Figure(a)). One

such figure(b) is marked with borders to indicate the ordered region. The remaining HRTEM images in the following sections are captured without any tilt angle.

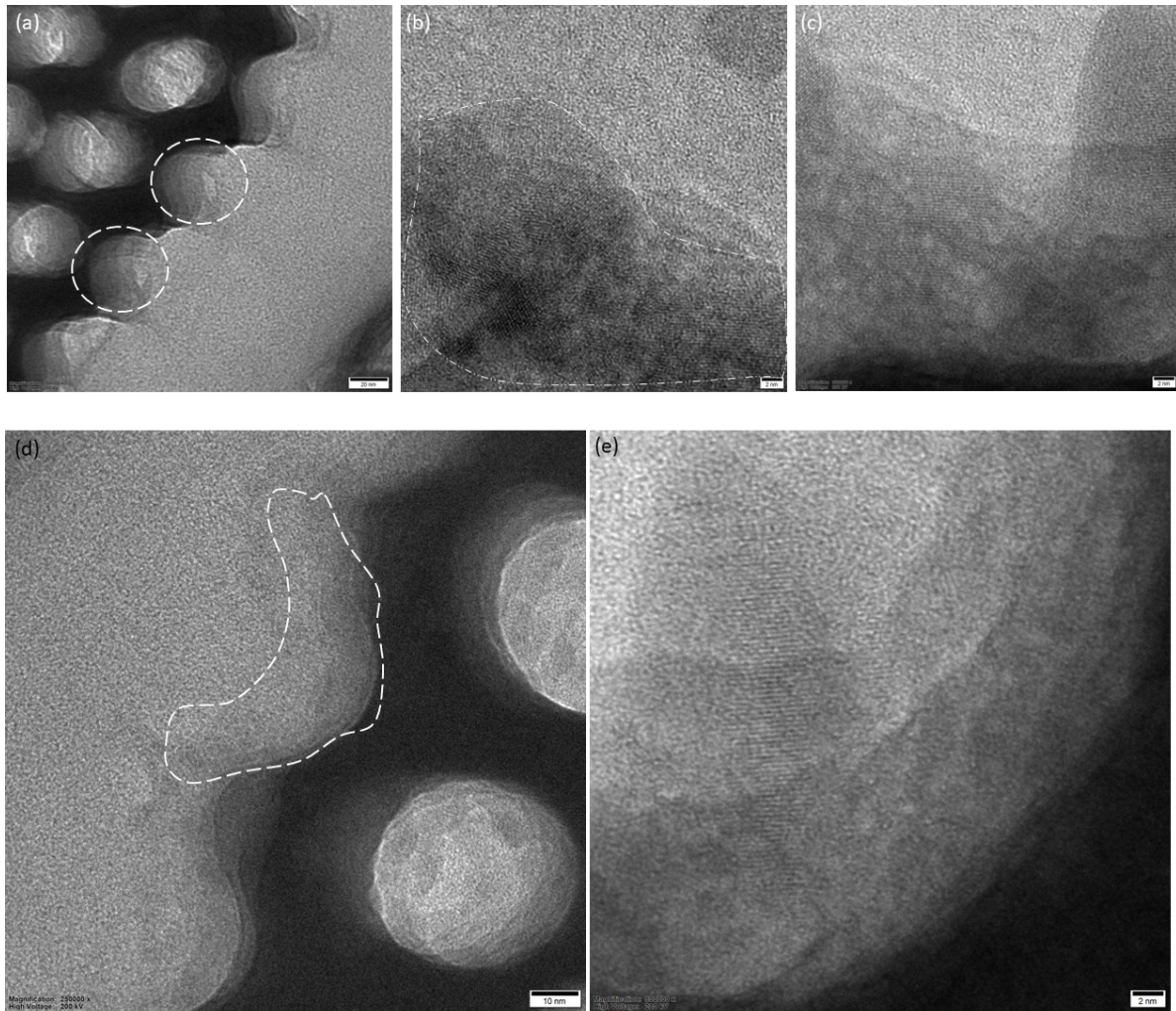
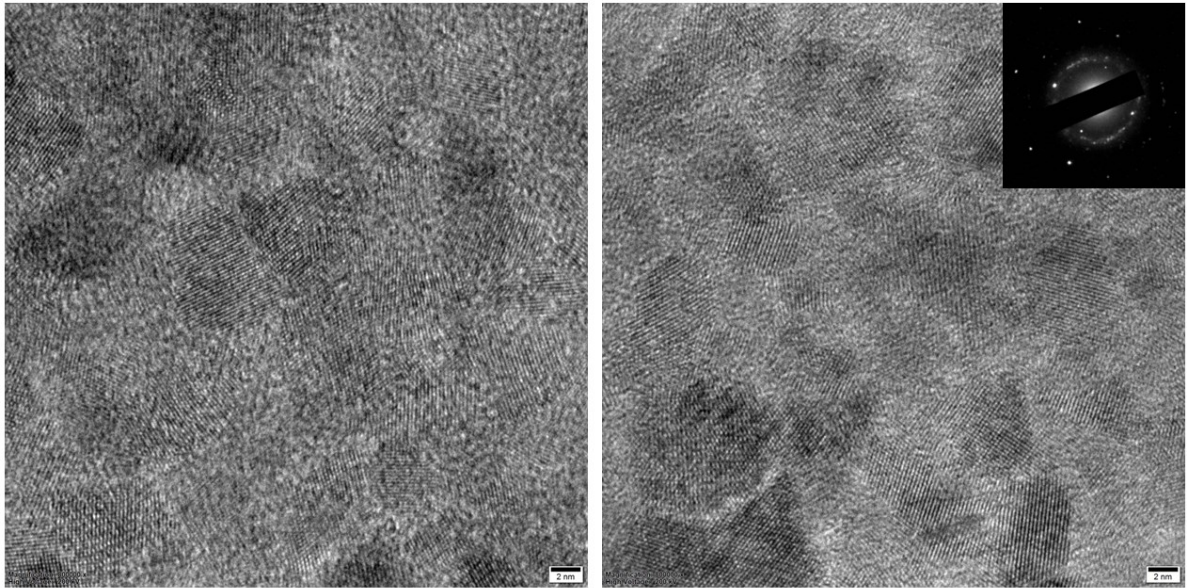


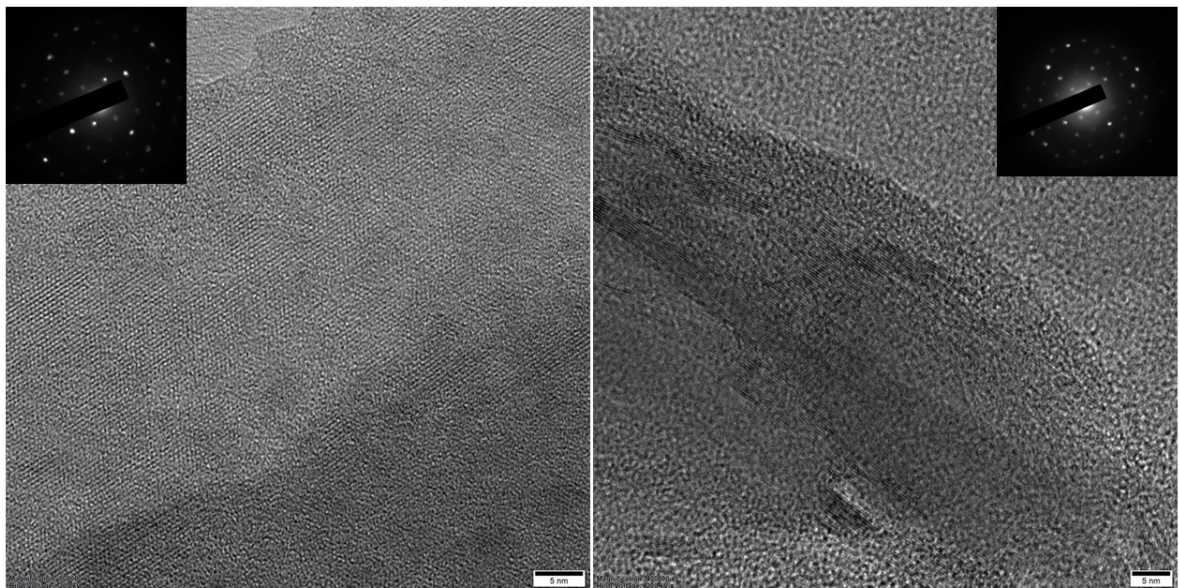
Figure S2. HRTEM of PEDOT:PSS at tilt angle  $\sim 10^\circ$ .

### 3. HRTEM imaging and SAED patterns for different PEDOT-samples in bulk films

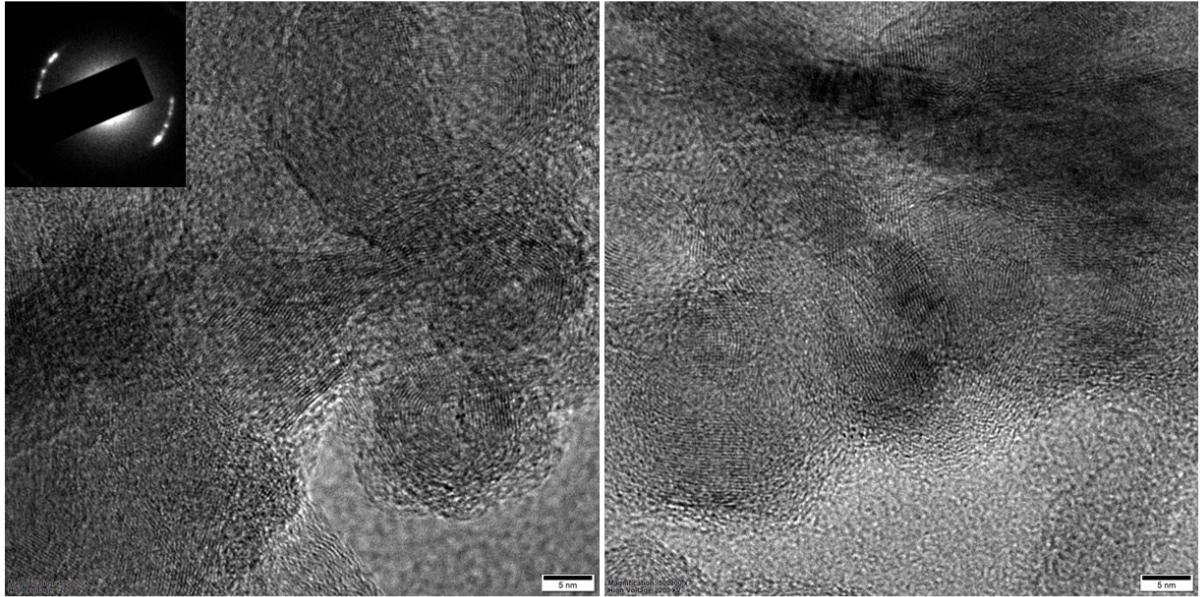
PEDOT:Tos films



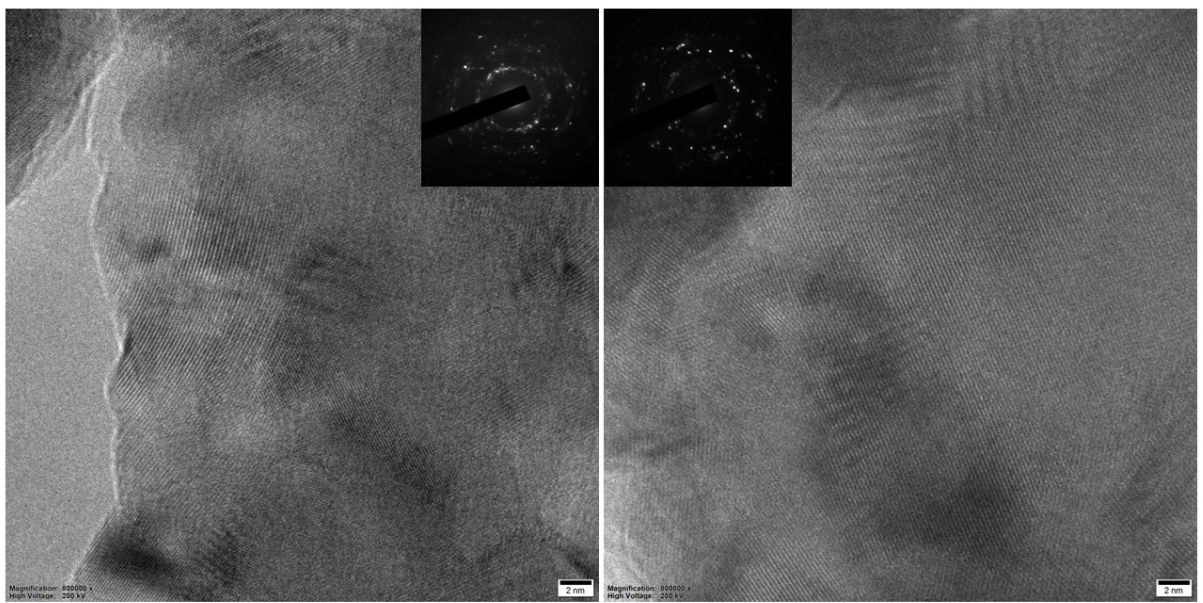
Spin-coated PEDOT:PSS mix



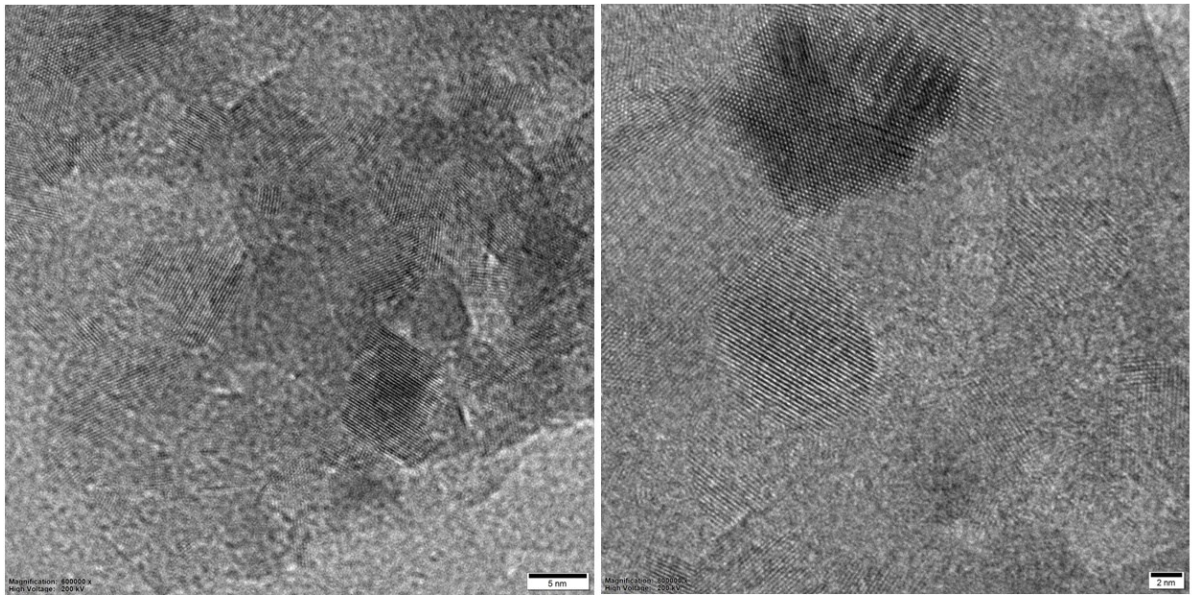
Spin-coated PEDOT:PSS (1:2.5)



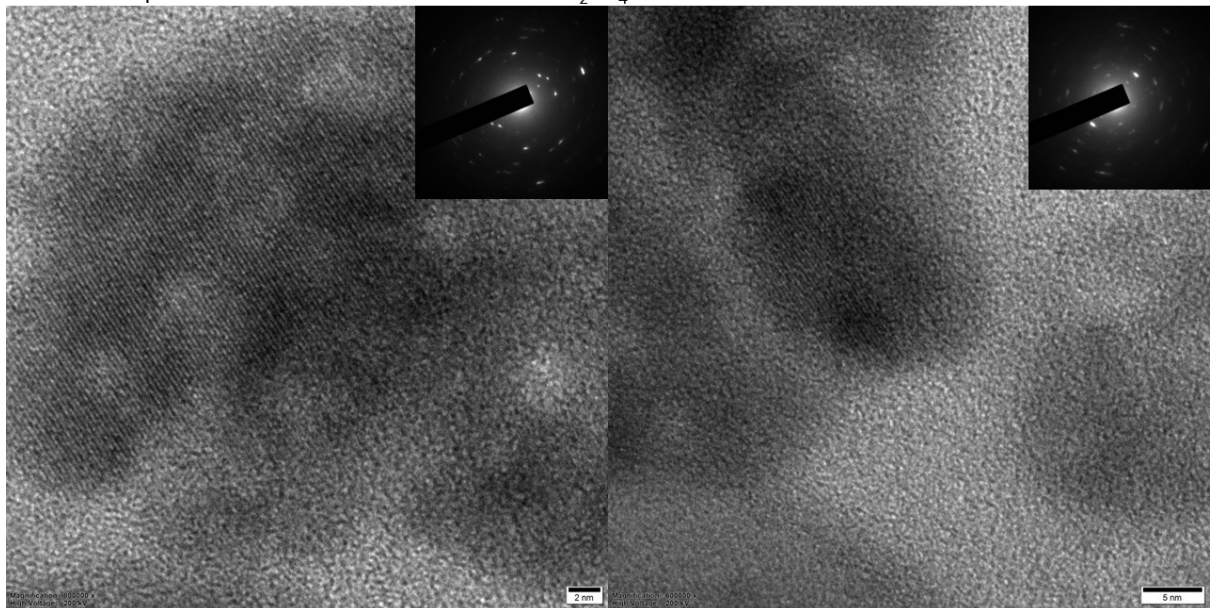
Spin-coated PEDOT:PSS (untreated)



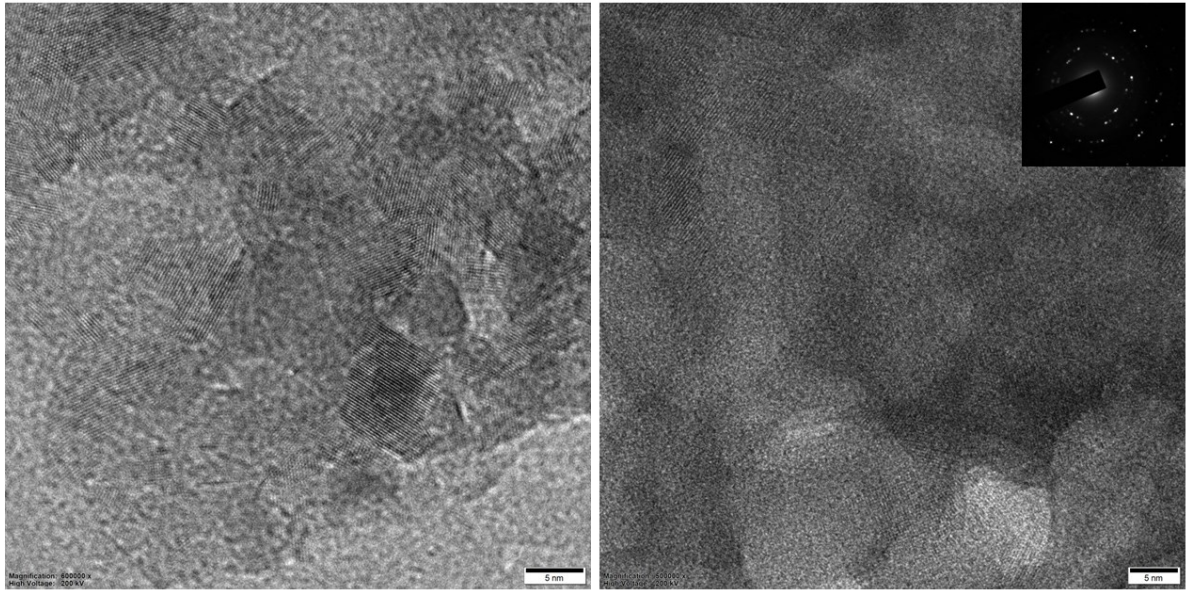
Spin-coated PEDOT:PSS\_1:6 and acid treated  $H_2SO_4$



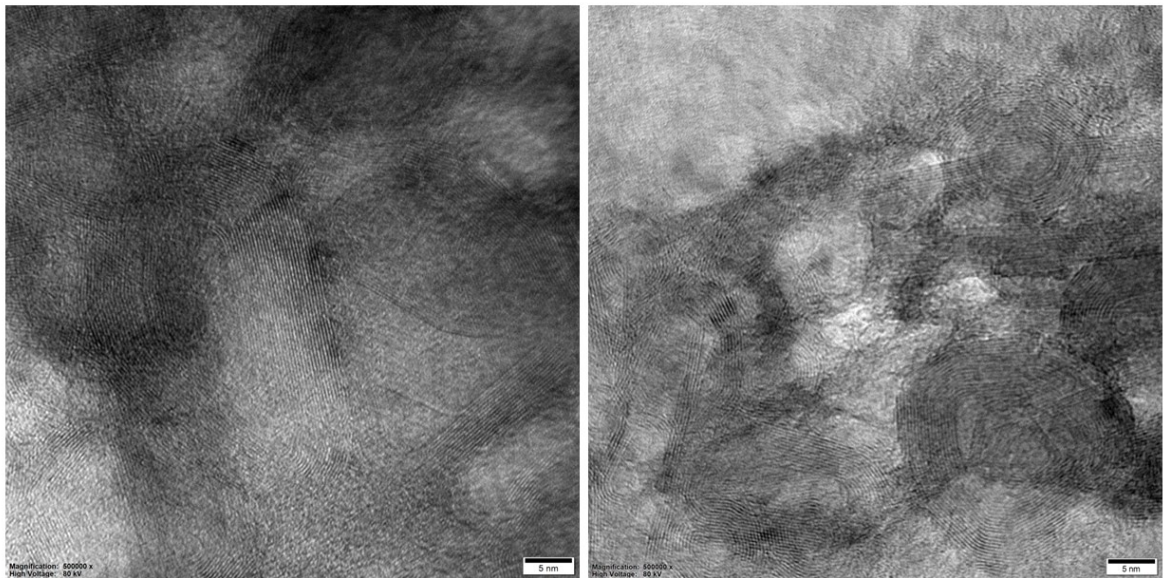
Drop-casted PEDOT:PSS and acid treated  $H_2SO_4$



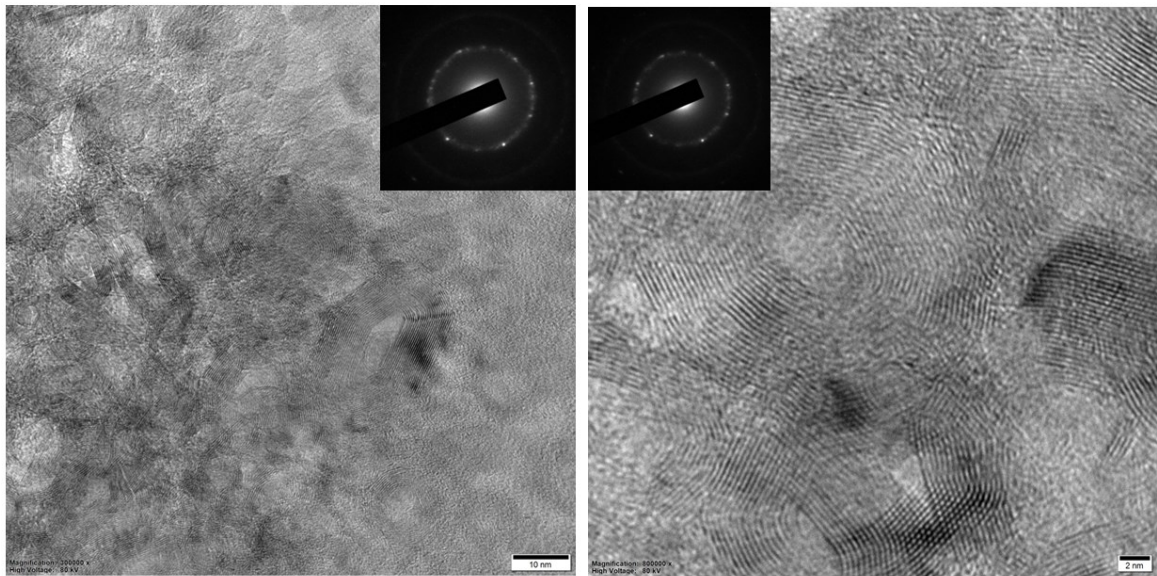
Spin-coated PEDOT:PSS (untreated)



Drop-casted PEDOT:PSS (untreated)



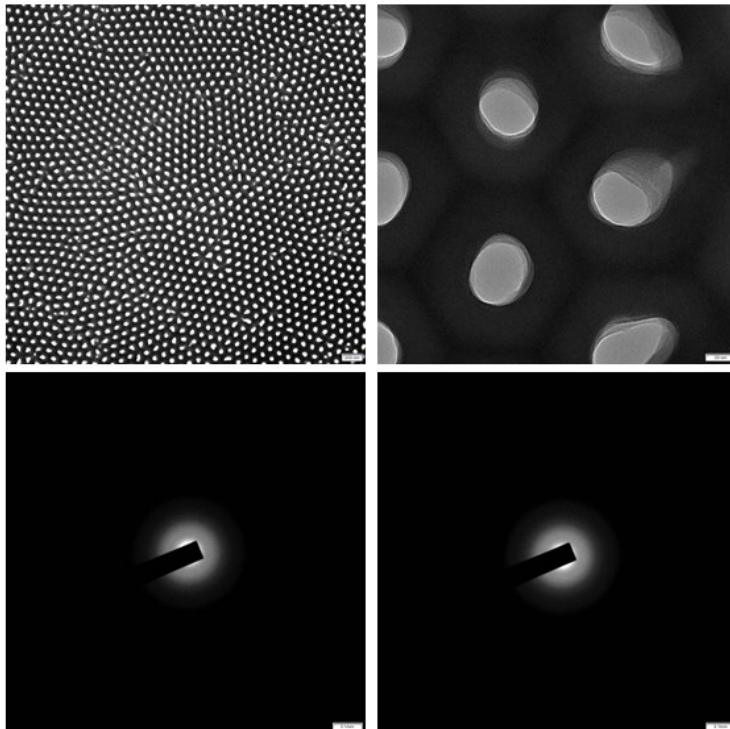
Drop-casted PEDOT:PSS (untreated)



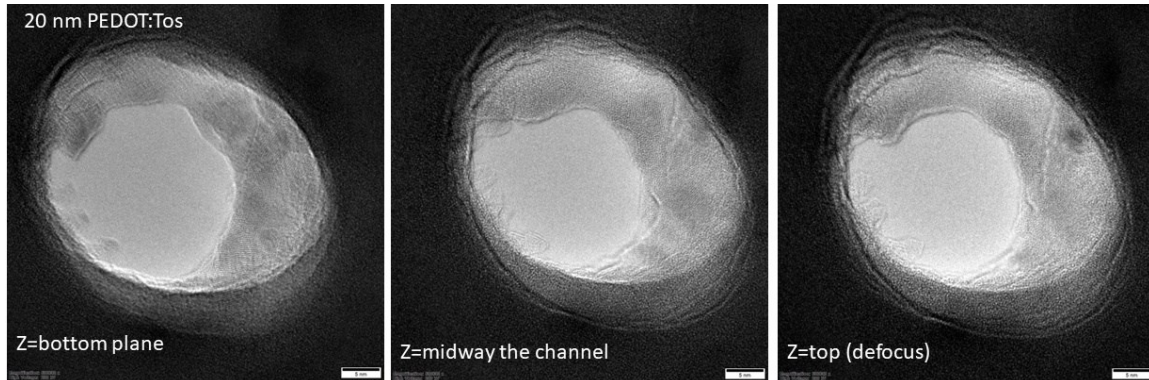
4. HRTEM imaging and SAED patterns from different PEDOT nanochannels of channel diameters 20 nm, 50 nm and 80 nm.

Amorphous structure of alumina, no diffraction observed.

Only AAO-no polymer  
Amorphous region of nanochannels



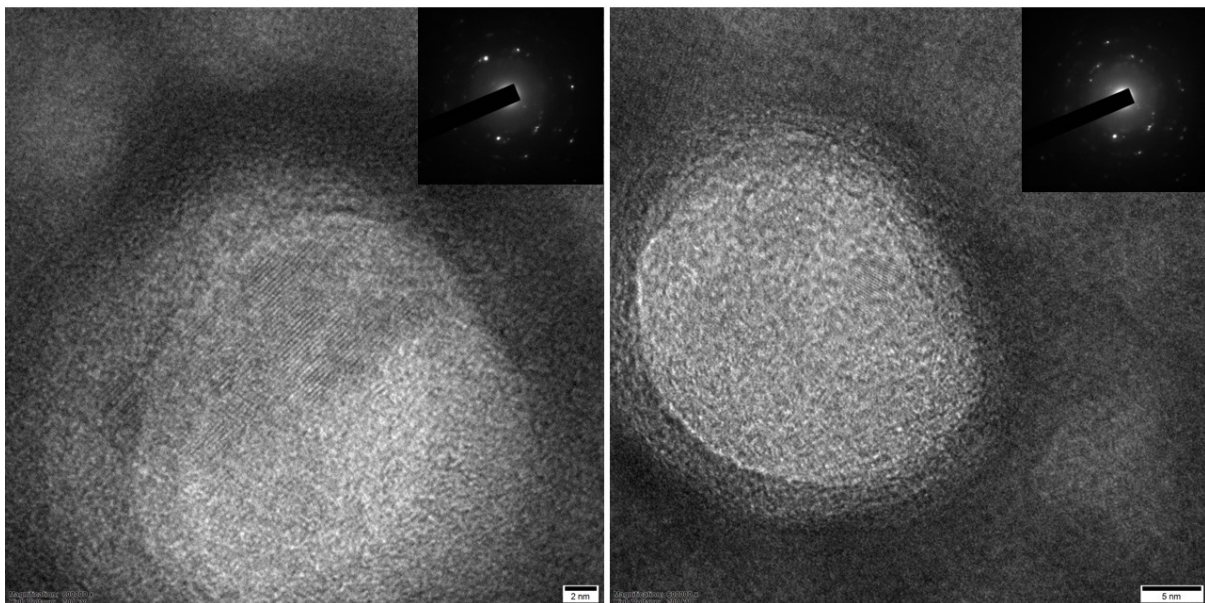
In all the following images, different proportion filling of PEDOT inside the nanochannels are imaged to highlight the ordering of chains inside, on the walls and outside the nanochannels.



The HRTEM images show the filling of polymer along the height of AAO. This is confirmed by changing the defocus length and capturing HRTEM from different planes.

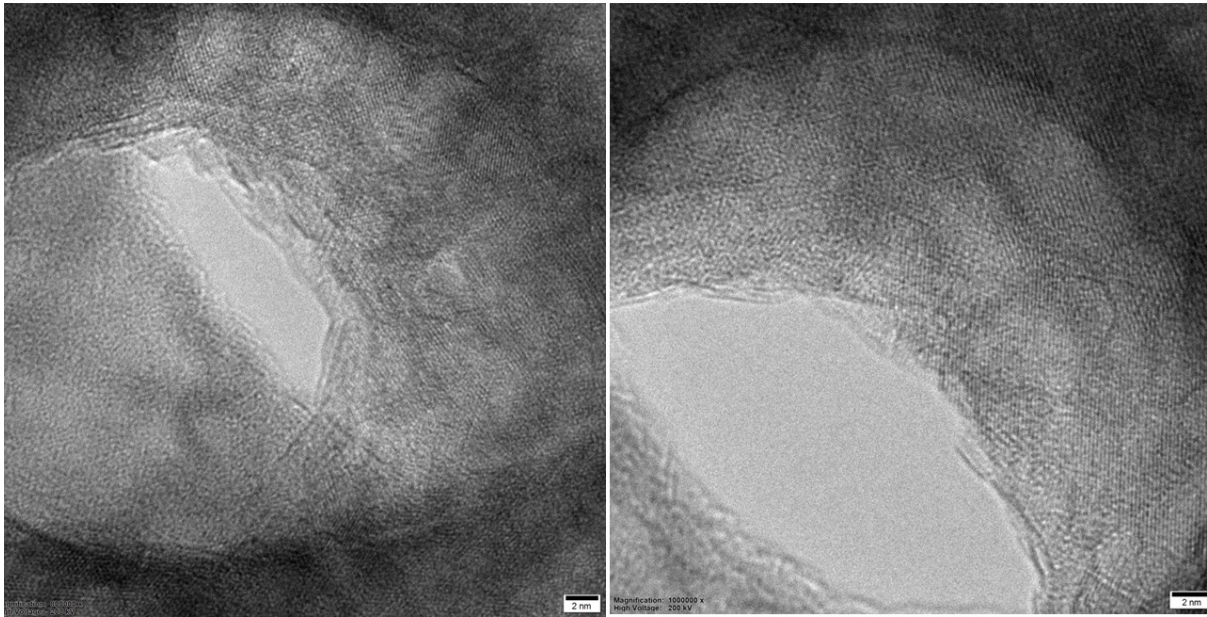
HRTEM and SAED patterns:

20 nm PEDOT:PSS nanochannels

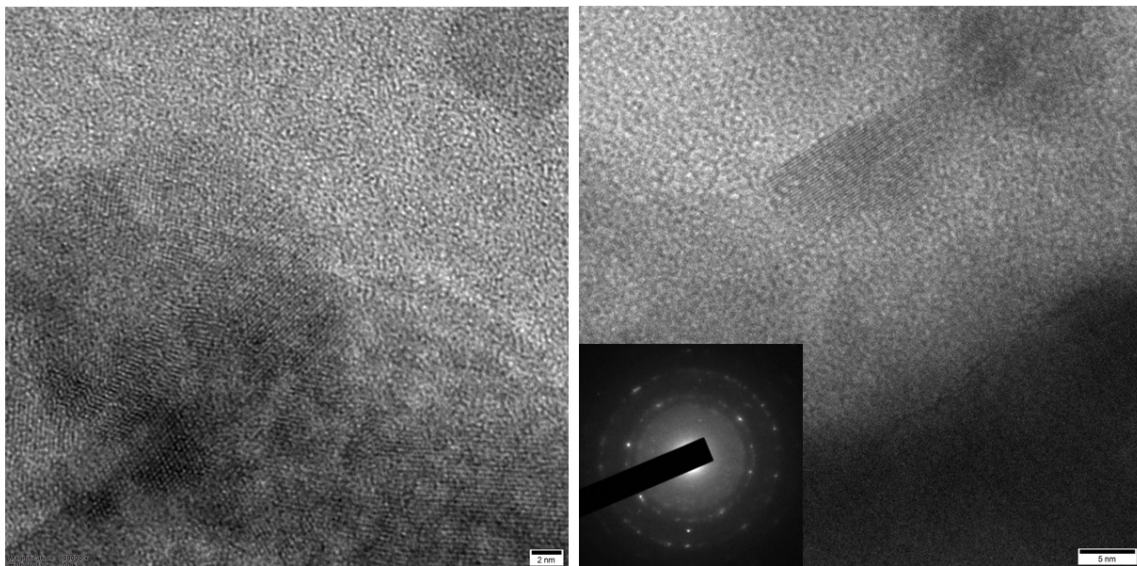


Ordering of PEDOT along the walls of nanochannels.

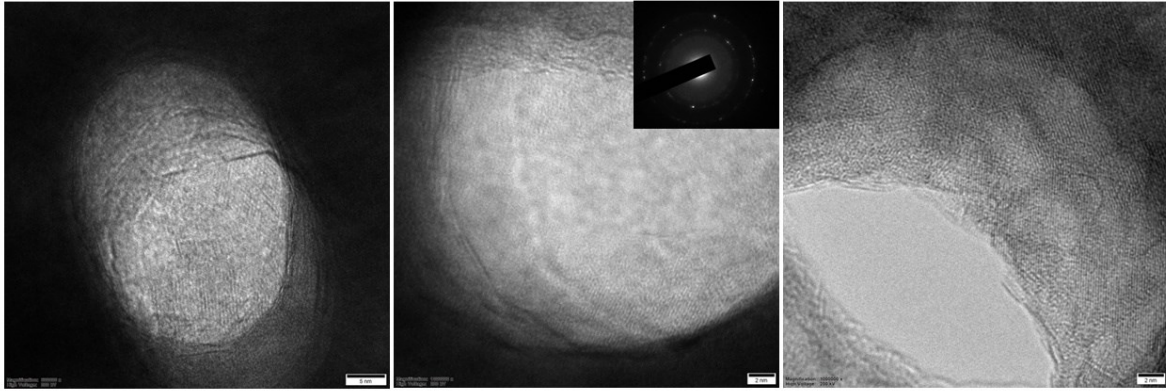
20 nm PEDOT:PSS nanochannels



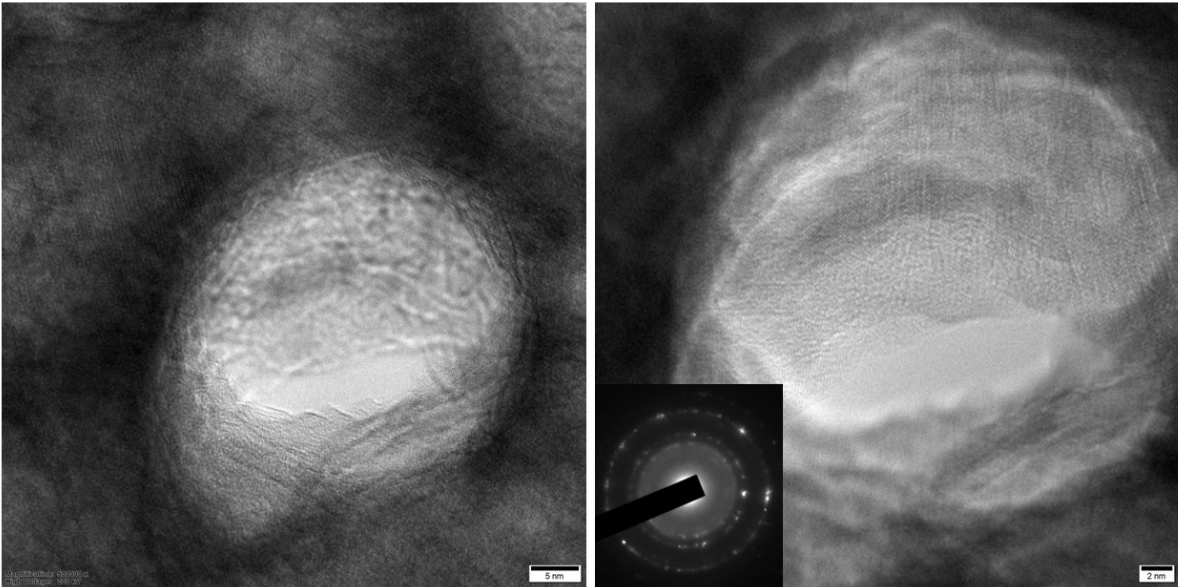
20 nm PEDOT:PSS\_1:2.5 and acid treated nanochannels



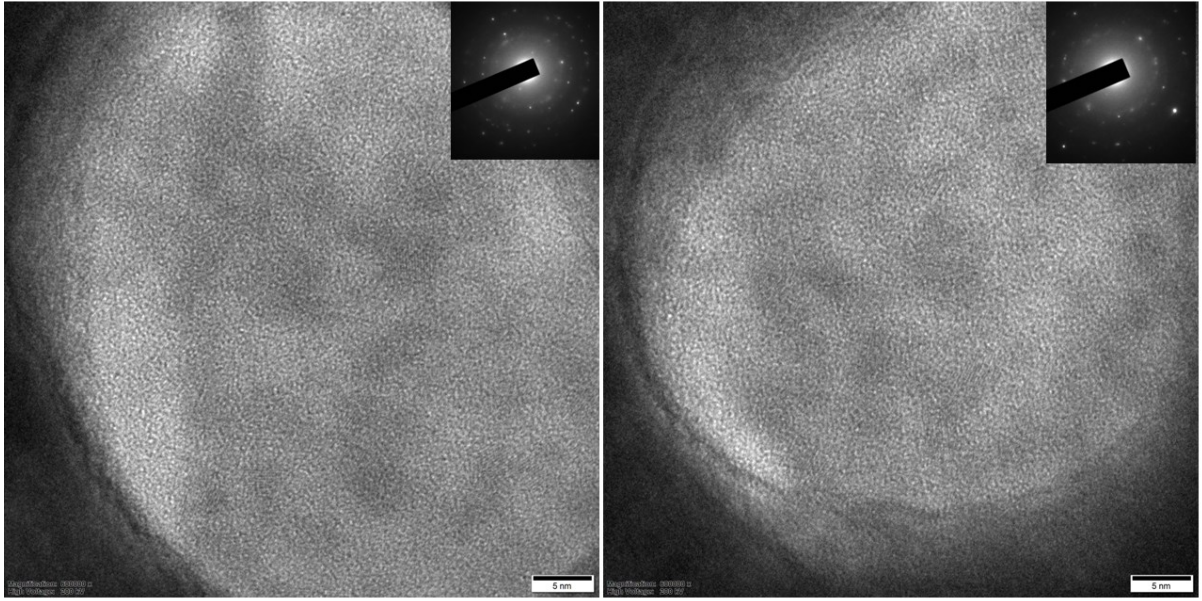
20 nm PEDOT:PSS nanochannels with acid



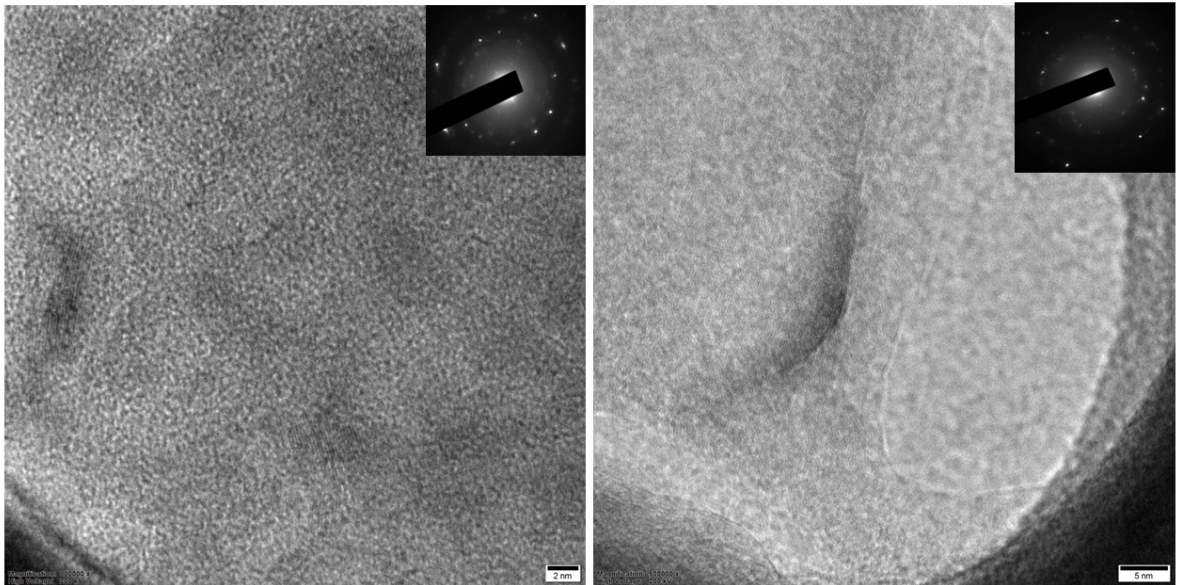
20 nm PEDOT:PSS\_mix nanochannels



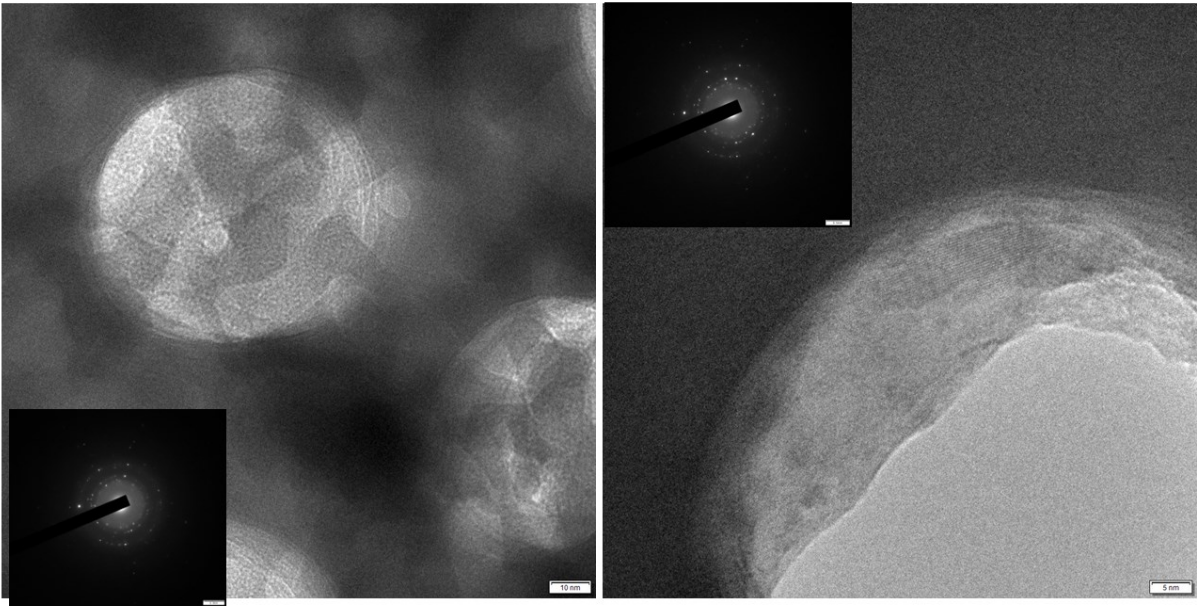
50 nm PEDOT:PSS



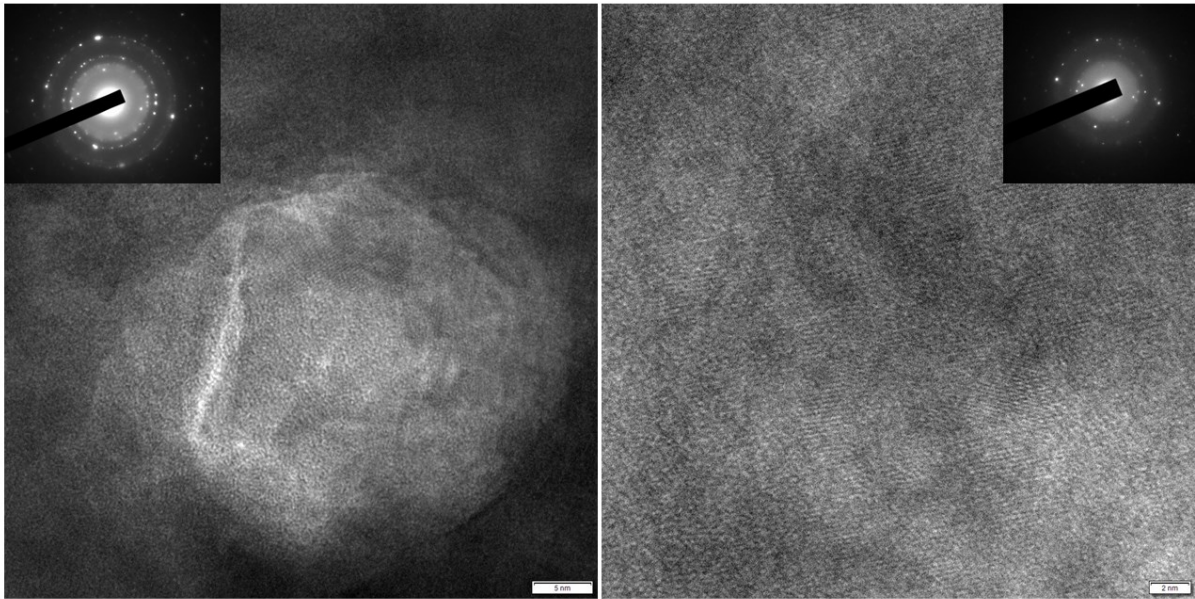
80 nm PEDOT:PSS



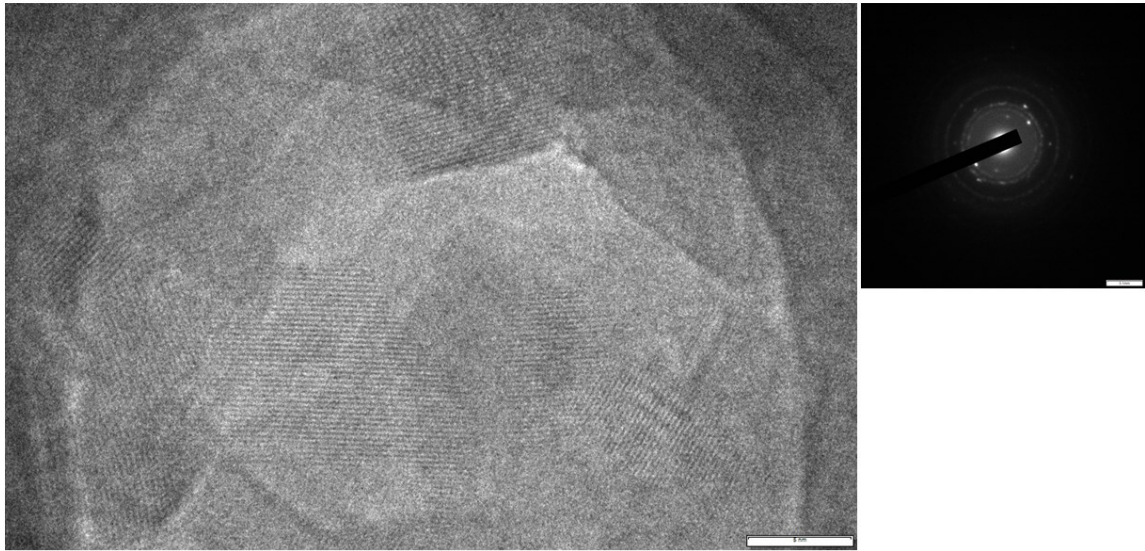
80 nm PEDOT:Tos nanochannels



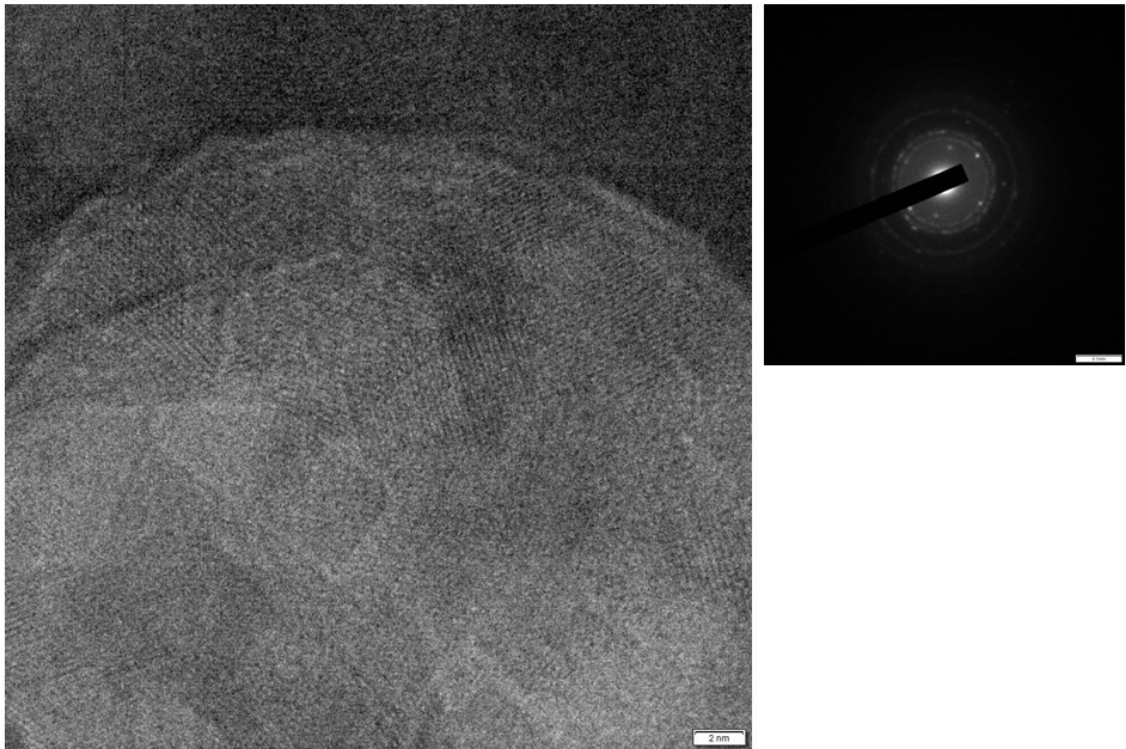
50 nm PEDOT:Tos nanochannels



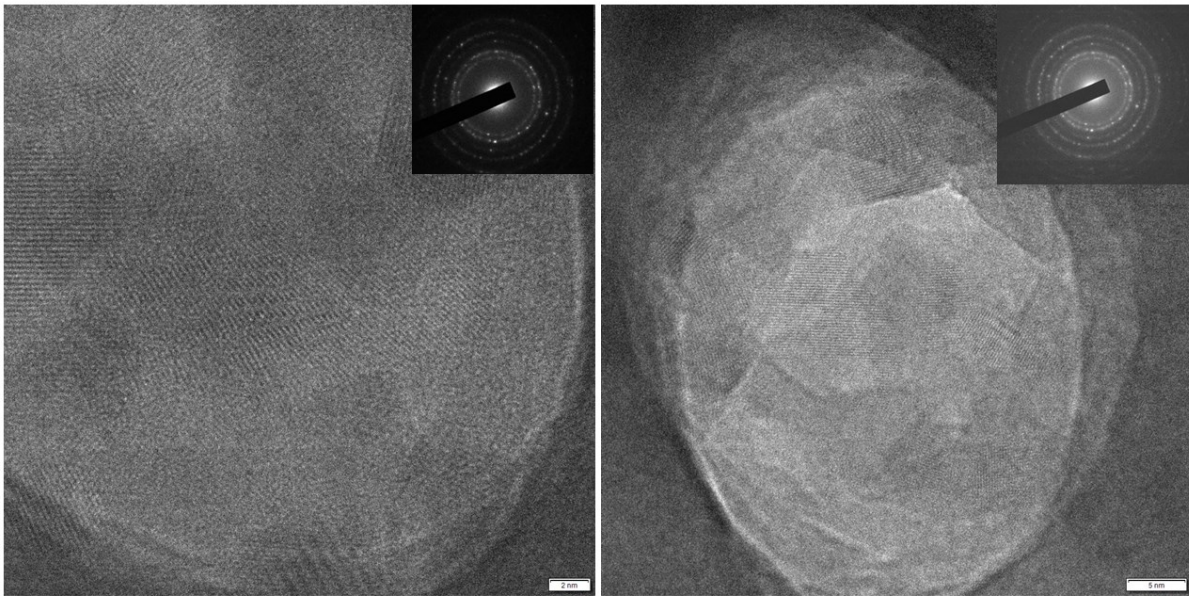
20 nm PEDOT:Tos nanochannels



20 nm PEDOT:Tos nanochannels



## 20 nm PEDOT:Tos nanochannels



All the HRTEM have been provided to the maximum possible resolution such that the fringes and ordering of PEDOT domains are visible.

### 5. AFM surface morphology of acid treated PEDOT:PSS surfaces

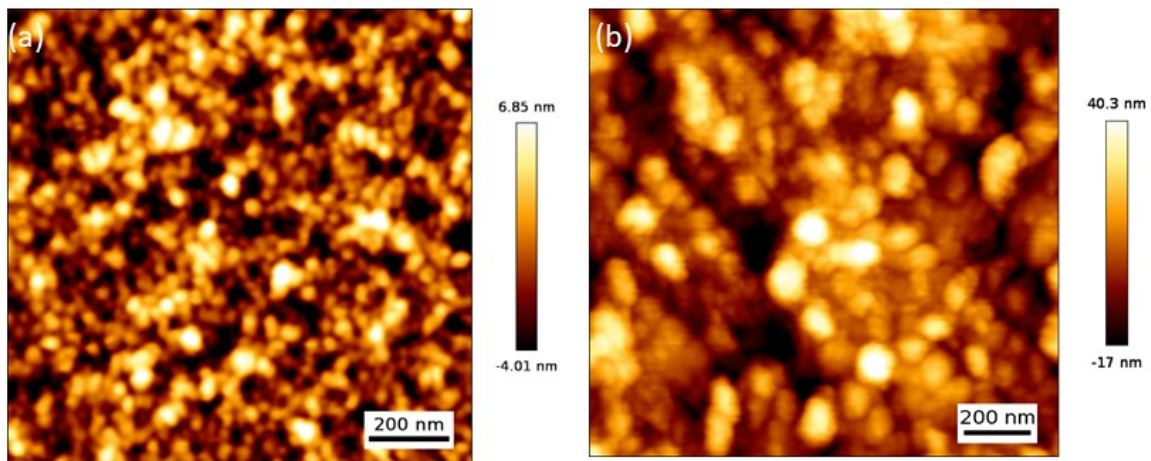


Figure S5. (a) Bulk thin films without and (b) with acid treated surfaces. Roughness increases with acid treatment on PEDOT:PSS surfaces.

### 6. Atomic Force Spectroscopy

The force mapping with contrasting force magnitudes from porous and nonporous region in AAO sample was not seen clearly. This was because the adhesion forces between the adjacent

regions (pore and nonpore) were not adequately distinct in PEDOT AAO samples and thus we couldn't perform force mapping unlike CAFM which showed contrasting dark and bright current magnitudes. Higher PSS ratios have low contact angles and high adhesive factors. PEDOT:Tos in different nanochannels are not significantly different (Figure S6e and S6f).

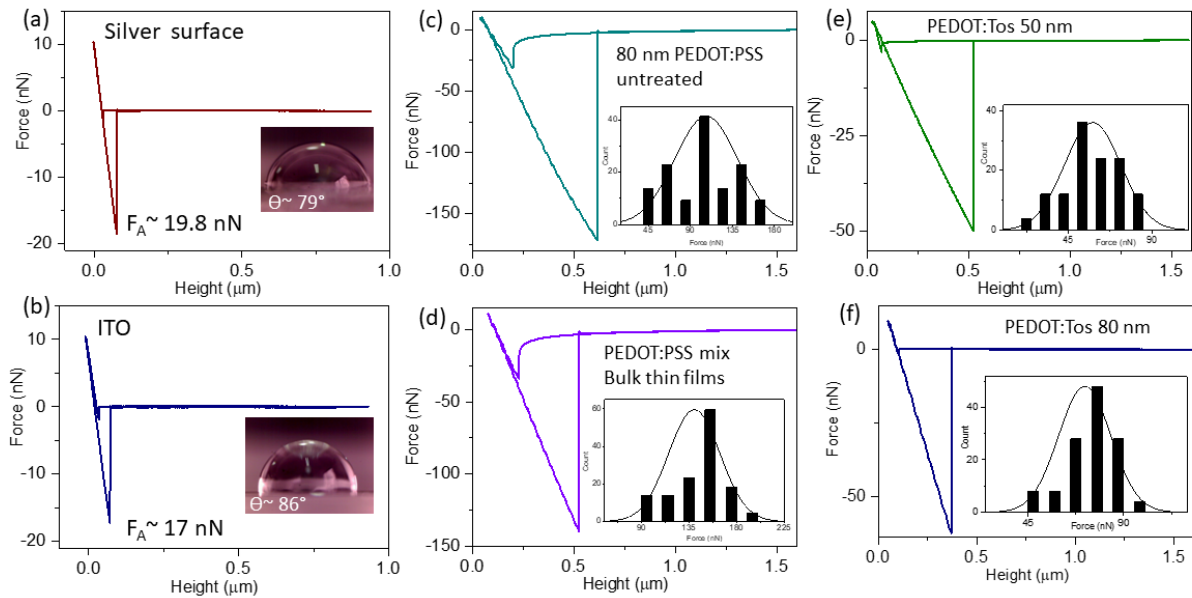


Figure S6. Force spectroscopy using 20 nm radius of curvature Pt/Ir coated AFM tip on (a) Silver (b) ITO (c) 80 nm PEDOT:PSS (untreated), (d) PEDOT:PSS mix bulk thin films (e) PEDOT:Tos 50 nm and (f) PEDOT:Tos 80 nm film surfaces at the point of contact of film and tip. (Insets of a,b indicate the contact angle measurements of water with corresponding surfaces at macroscopic level).

## 7. MD simulation results

In the case of the 5 nm PEDOT:PSS system (see **Figure S7**), the XRD peaks are not so pronounced due to the presence of very few PEDOT chains in such a small diameter nanochannel as the confinement is too high. As the diameter increases, it allows more PEDOT chains to accommodate inside the nanochannel and hence, the peaks become more prominent.

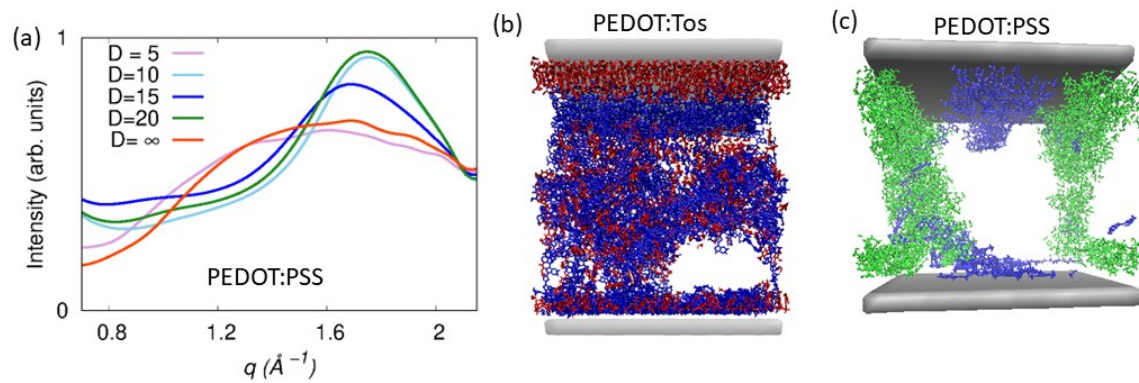


Figure S7. (a) XRD distribution functions of PEDOT chains plotted for PEDOT:PSS. Polymers equilibrated between AAO slabs (b) PEDOT:Tos and (c) PEDOT:PSS.